Machine Learning Techniques as a Helpful Tool Toward Determination of Plaque Vulnerability

Myriam Cilla, Javier Martínez, Estefanía Peña, and Miguel Ángel Martínez*

***Abstract*—Atherosclerotic cardiovascular disease results in millions of sudden deaths annually, and coronary artery disease accounts for the majority of this toll. Plaque rupture plays main role in the majority of acute coronary syndromes. Rupture has been usually associated with stress concentrations, which are determined mainly by tissue properties and plaque geometry. The aim of this study is develop a tool, using machine learning techniques to assist the clinical professionals on decisions of the vulnerability of the atheroma plaque. In practice, the main drawbacks of 3-D finite element analysis to predict the vulnerability risk are the huge main memories required and the long computation times. Therefore, it is essential to use these methods which are faster and more efficient. This paper discusses two potential applications of computational technologies, artificial neural networks and support vector machines, used to assess the role of maximum principal stress in a coronary vessel with atheroma plaque as a function of the main geometrical features in order to quantify the vulnerability risk.**

***Index Terms*—Artificial neural network (ANN), coronary disease, parametric finite element analysis, support vector machine (SVM).**

I. Introduction

CARDIOVASCULAR diseases related to atherosclerosis are the first cause of death in the western world; more people die annually from cardiovascular diseases than from any other cause [1]. This relevant fact has motivated the development of numerical models for arterial behavior in order to understand better cardiovascular pathologies. The use of finite element methods (FEMs) for the analysis and design of bioengineering processes often requires long computational time cost; the simulation time can be significantly reduced combining this technique with machine learning techniques.

Atherosclerosis is a diffuse disease process that results in the accumulation of fatty, fibrous, calcific, and inflammatory tissue within the arterial wall. As an atheromatous lesion expands, it causes narrowing (stenosis) of the arterial lumen, hardening of the arteries, and loss of their elasticity. Furthermore, the worst damage occur if the plaque becomes fragile and ruptures (vulnerable plaque). The final result is myocardial infarction, stroke, or organ failure [1].

Over the past years, various methods have been used to quantify atherosclerosis: invasive methods such as intravascular ultrasound (IVUS), and noninvasive methods, like X-ray angiography, both based on the detection of classical risk factors [2]. Identifying vulnerable patients before plaque rupture occurs would help clinicians to provide early treatment taking preventive measures. The term "vulnerable patient" is proposed for the identification of individuals with a high likelihood of developing cardiac events in the near future [3]. Despite major advances on the treatment of coronary artery disease, the available screening and diagnostic methods are insufficient to identify the victims before the event occurs.

Regarding the mechanical forces, some authors [4] consider peak circumferential stress as the most important biomechanical factor in the mechanisms leading to rupture of the atherosclerotic plaque and it has often used as a predictor of atherosclerotic plaque rupture location. Traditionally, only the fibrous cap thickness and the stenosis ratio have typically been identified as the key predictor of vulnerability and likelihood of rupture, and, generally, the clinical staff identify the vulnerable plaque just based on these parameters. However, some clinical and biomechanical studies [5]–[7] shown that the fibrous cap thickness alone is not a sufficiently accurate predictor for plaque stability. The lipid core length and width are also very important and influential parameters on maximal principal stress (MPS). Thus, these parameters should also be measured during the clinical test.

Procedures to detect plaque prone to rupture and to predict rupture location are very valuable for clinical diagnosis. Nowadays, clinical procedures for detection of these vulnerable plaques are only performed by image analysis. The use of FEM computations presents the disadvantage of very high computational cost, usually hours or even days, when an immediate response is required. However, FEM analysis is used in preoperatory surgical planning when clinical staff have enough time to perform the computational model and analyze the results. The main objective of this paper is to search for alternatives to direct FEM simulations in a specific clinical field, detection of

vulnerable plaques, when an instantaneous response is needed. Thus, this paper focuses on the uses of different machine learning techniques, such as artificial neural networks (ANNs) and support vector machines (SVMs), applied to study the role of stress in plaque vulnerability in order to reduce the very long computation times and memory consumption required for 3-D finite element (FE) analysis. The clinical validation of these results is out of the scope of this paper. The SVMs [8] give rise to a new class of theoretically elegant learning machines that use a central concept of SVMs—kernels—for a number of learning tasks. Kernel machines provide a modular framework that can be adapted to different tasks and domains by the choice of the kernel function and the base algorithm [9]. Multilayer perceptron (MLP), as a representation of the ANNs, is a feed-forward network characterized by its layered structure, each layer consisting of a set of perceptron neurons and its training algorithm [10]. These techniques have been previously used by researchers to solve different classification and regression engineering problems [11]–[13].

The machine learning techniques use an intelligent algorithm to model the atheroma plaque rupture in terms of four of the most influential geometrical factors in the plaque rupture: 1) fibrous cap thickness; 2) stenosis ratio; 3) lipid core width; and 4) lipid core length. The output predicted is the maximum MPS occurred in an atherosclerotic coronary vessel with the input dimensions. For this purpose, an idealized and parametric coronary vessel model has been performed using FEM in order to train the machine learning.

The ultimate goal of this paper is to develop a quantitative method for cumulative risk assessment of vulnerable patients based on atheroma plaque morphology which could replace the time-consuming biomechanical simulations used in cardiovascular mechanics. Summing up, the procedure proposed would be carried as follows: for a specific patient, clinical staff should measure just four parameters in standard IVUS images, and then, by using the ANN or SVM techniques, they would have an immediate response on the atheroma plaque vulnerability. Parametric FEM analysis would have been performed before in order to feed the ANN or SVM algorithms and the database. Furthermore, a comparison of the performance of SVMs and ANNs is provided. To the best of the authors knowledge, this is the first publication concerning this kind of analysis. A parametric tool based on machine learning techniques, used to predict the atheroma plaque rupture, has not yet been carried out.

II. Atheroma Plaque Problem

A. 3-D Parametric Study

A 3-D parametric study of the geometric factors used to check the vulnerability of atherosclerotic plaque was performed. A 3-D idealized geometry corresponding to a coronary vessel with atheroma plaque was modeled. Such plaques are characterized by a large lipid pool with a thin fibrous cap [14]–[16]. Atherosclerotic vessel morphology and average dimensions were obtained from Versluis *et al.* [4] and Bluestein *et al.* [17]. A vessel length of 20 mm, external radius of 2 mm, and vessel wall thickness of 0.5 mm were considered as basis geometry. A 3-D

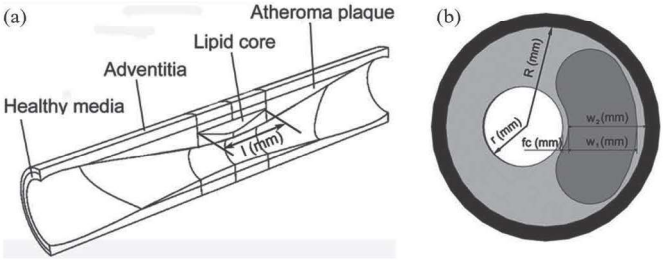

Fig. 1. (a) Idealized geometry of an atherosclerotic arterial model. Transversal section. (b) Geometrical parameters shown on the cross central section of the atherosclerotic vessel.

FEM was developed using the commercial FE code ABAQUS 6.9, taking into account both the composition and dimensions of the different layers of the tissue (media and adventitia), the fibrous plaque, and the lipid core.

The arterial wall was approximated as a hollow cylinder with a circular lumen. The atherosclerotic plaque was modeled as a symmetric volume with respect to the central cross section (longitudinal axis), located inside the vessel. Finally, the lipid core was approximated as a blunt volume (see Fig. 1). In areas with atheroma plaque, the whole media layer was considered as fibrotic, whereas only the adventitia was considered as a healthy layer. All tissues were considered to be nonlinear, hyperelastic, and incompressible materials [18]. The behavior of the tissue was modeled by the Gasser, Ogden, and Holzapfel strain energy function [19]. In order to obtain the material parameters for the constitutive law of the tissue, experimental data presented in previous works (adventitia and media properties from Holzapfel *et al.* [18] and plaque and lipid core properties from Versluis *et al.* [4]) were fitted using the Levenberg–Marquardt minimization algorithm [20].

Regarding the boundary conditions, the longitudinal displacements were constrained at the end of the vessel, whereas the radial displacement was allowed. Symmetry conditions were imposed in the corresponding symmetry planes. In order to introduce the longitudinal residual stress, the model was stretched a 4.4% of the vessel length (longitudinal direction), representing *in vivo* conditions [18]. Then, a constant internal pressure of 140 mmHg (18.7 kPa) was imposed in the inner surface of the lumen, simulating the blood flow pressure [21].

The parametric model consists of a series of idealized plaque morphology models, mimicking different stages and variations in atherosclerotic lesion growth. According to previous works [7], [16], [21]–[23], the most influential geometric parameters considered were fibrous cap thickness (*fc*), stenosis ratio (*sr*), which is obtained by dividing the lumen radius by the lumen radius of a normal artery ($R = 1.5$ mm), $\mathrm{sr}(\%) = \frac{r(\mathrm{mm})}{R(\mathrm{mm})}100$, lipid core length l, and lipid core width w. Lipid core width w was defined as the ratio between the percentage of the atheroma plaque width w_1 and the distance from the inner point of the lipid core to the outer point of the fibrotic plaque w_2, $w(\%) = \frac{w_1(\mathrm{mm})}{w_2(\mathrm{mm})}100$. The central section of the 3-D model is shown in Fig. 1(b) where the lipid core length was measured in the perpendicular direction [see Fig. 1(a)].

TABLE I
VARIATIONS OF THE GEOMETRICAL PARAMETERS ANALYZED

Level	l(mm)	sr(%)	fc(mm)	w(%)
1	1	46.7	0.025	30
2	2	53.3	0.05	45
3	4	56.7	0.1	60
4	6	60	0.15	75
5	8	66.7	0.25	90

Five variations or levels for each parameter were considered with a total of $5^4 = 625$ idealized eccentric vessel models with atherosclerotic lesions. Realistic morphological data were investigated by varying lipid core length (1 mm $\leq l \leq$ 8 mm), stenosis ratio ($46.7\% \leq$ sr $\leq 66.7\%$), fibrous cap thickness (0.025 mm $\leq fc \leq$ 0.25 mm), and lipid core width ($30\% \leq w \leq 90\%$) [24]. The different level values of the geometrical parameters used to define the idealized coronary plaque models are included in Table I.

B. Source Data

MPS was considered as the mechanical factor for the purpose of comparison in the parametric study in order to define vulnerability risk.

Regarding the vulnerability of the plaque, different threshold stress values have been proposed by several authors [22], [25]. In this study, a threshold value of 247 kPa has been used according to the set of experimental data obtained by Loree *et al.* [25], supposing a normal distribution of the data. This threshold value indicates that the probability of having plaque rupture is 0.95 for the cases whose combination of parameters have maximum MPS equal or higher than 247 kPa.

Maximum MPS for each combination of parameters is shown in Fig. 2. The two most influential parameters, fibrous cap thickness and lipid core width, fc and w, were chosen as the variables represented by the surfaces approximation. In each subfigure, five surfaces are presented, one for each l variation, where the safety threshold plane at 247 kPa is presented [25]. The geometrical parameters and MPS represented in Fig. 2 were selected as inputs and output, respectively, to predict the atheroma vulnerability risk using ANNs and SVM methods.

III. MATHEMATICAL METHODS FOR REGRESSION

In the following sections, we briefly present the methods that are used in our comparative study. The machine learning techniques are concerned with the design and development of algorithms that allow computers to evolve behaviors based on empirical data.

A. ANN

ANNs are mathematical models that are inspired by the structure and functional aspects of biological neural networks [26]. It is a useful and robust computational tool for prediction which can acquire, store, and utilize experimental knowledge.

This model consists of two basic elements.

1) A structure consisting a set of basic units, called neurons, organized in layers. The network consists of three layers: input, hidden, and output. Each unit consists of the following neuronal components.
   a) A set of input connections, along with a set of weights that regulate the input signals intensity.
   b) The activation threshold, which is subtracted from the aggregation of the input signals transmitted.
   c) An activation function which focuses on the input signals.
   d) The output of the neuron as a function of the input signals, called transfer function.

   This structure is often called the network architecture, being able to make a classification of the networks as a function of the number of networks layers, the interconnection degree of the structure, or according to the character of the connections.
2) A training algorithm for calibrating the network weights and other parameters as a function of deviations of the outputs provided by the network and the actual values.

When considering the network functional model, we focus on the feed-forward network (network architecture in which each layer is connected with the following forward direction only, so that it can be represented by an acyclic graph), with specific activation functions and weights. So, the network implements a function $\mathbf{f}: \mathcal{X} \subset \mathbb{R}^d \longrightarrow \mathcal{Y} \subset \mathbb{R}^c$ where d is the input space dimension and c is the output space dimension. The functions implemented by a network feed forward can be formulated by the following general model:

$$\begin{aligned} \mathbf{f}(\mathbf{x}) &= \varphi(\psi(\mathbf{x})) = (\varphi \circ \psi)(\mathbf{x}) \\ \psi &: \mathcal{X} \subset \mathbb{R}^d \longrightarrow \mathcal{U} \subset \mathbb{R}^m \\ \varphi &: \mathcal{U} \subset \mathbb{R}^m \longrightarrow \mathcal{Y} \subset \mathbb{R}^c \end{aligned} \tag{1}$$

where $\mathcal{U}$ is the hidden variables space with dimension m (number of neurons of this layer), and it is called feature space. A particular case of neural networks is the MLP with a layered structure where each neuron is a perceptron. Thus, based on the architecture defined previously for the case of MLP [10] (see Fig. 3), we have

1) $\psi_j(\mathbf{x}) = \psi(\mathbf{w}_j^T \mathbf{x} + w_{j0})$ with ψ being the hidden layer activation function, $\mathbf{w}_j \in \mathbb{R}^d$ being the parameter vector of the hidden layer, and $w_{j0} \in \mathbb{R}$ is its threshold value. The function ψ can be a sigmoid, a logistic, or a hyperbolic tangent.
2) $\varphi_j(\mathbf{u}) = \varphi(\mathbf{c}_j^T \mathbf{u} + c_{j0})$ with φ being the output layer activation function, $\mathbf{c}_j \in \mathbb{R}^m$ being the weights, and $c_{j0} \in \mathbb{R}$ is its threshold value. The activation function φ can be the identity function, Heaviside function, or any dichotomous function.

The sigmoid type and the linear functions have been selected for the hidden layer and the output layer, respectively, among all the possible transfer functions [10].

A typical feature of MLP is the training algorithm of back-propagation [10] which minimizes a combination of squared errors and weights starting from randomly distributed weights, and then determines the correct combination. Once an MLP is trained, it has input data fed into it, and from that, generates an

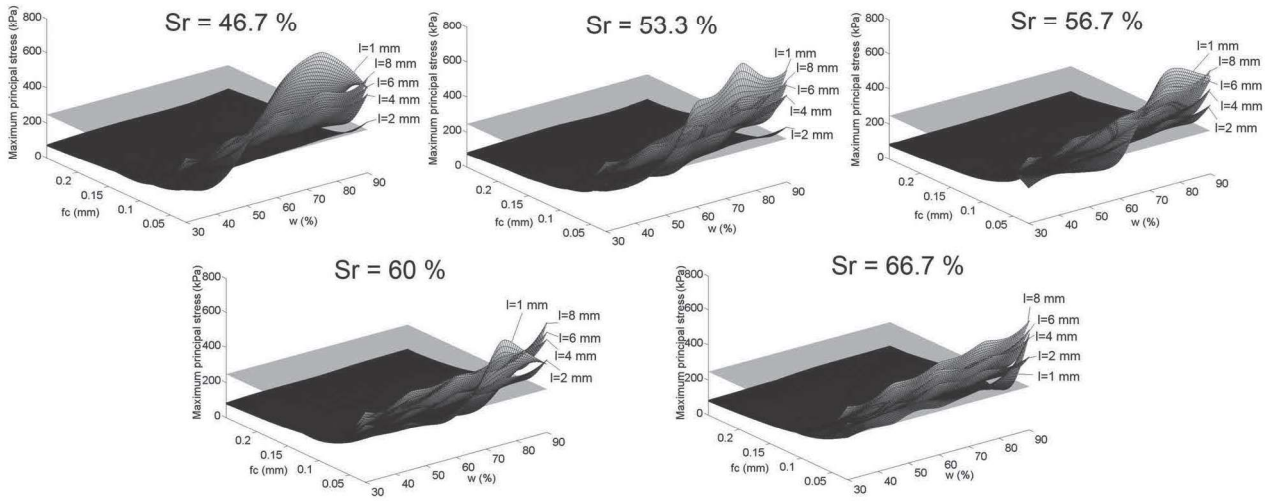

Fig. 2. Maximum MPS surfaces for a given stenosis ratio. Adapted from [7].

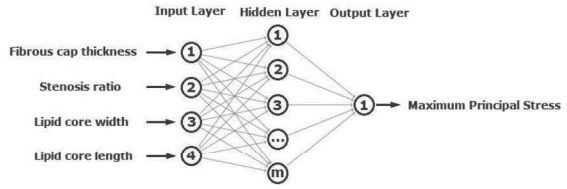

Fig. 3. ANN structure.

appropriate output. The structure of the MLP, combined with the nonlinearity and its weights, adjusted by the training algorithm, creates general function approximations that allow for the generation of practically any nonlinear function.

A cross-validation process was implemented in order to minimize the selection of the test set. The original set of training data is split into three groups: the first group consists of a training dataset with the 80% of the data patterns; the remaining groups are the validation dataset with 10% of the patterns and the remaining 10% of the data patterns are used to evaluate the performance of the MLP. The weight configuration for the best performance reached is stored and only replaced if a better performance has occurred. In this way, the best weight configuration can be determined. This process is repeated ten times (fold cross validation) [27].

B. SVM

Vapnik [8] is considered as the pioneer in introducing the concept of optimum separating hyperplane of a sample of data in a classification problem, which is the core of the SVM method (SVM).

Different historical facts can be highlighted in the development of SVMs.

1) The feature space generation from input space by the transformation $\psi : \mathcal{X} \subset \mathbb{R}^d \longrightarrow \mathcal{Z} \subset \mathbb{R}^s$ with $s \geq d$ (can be ∞). By the reverse transformation, the linear boundaries of the separating hyperplanes in the feature space result in nonlinear boundaries in the input space. This transformation is called the kernel trick.
2) The appearance of soft-margin algorithm for problems where perfect separability is not reachable (problems with noise in the sample data).
3) The SVM generalization to regression problems by way of Vapnik's ε-insensitive loss function [28].

Given a sample of data $\{(\mathbf{x}_i, y_i)\}_{i=1}^n$, the SVM problem [28] can be formulated as follows:

$$\min_{\mathbf{w},b,\boldsymbol{\xi}} \frac{1}{2}\left\{\left\|\mathbf{w}^2\right\| + C\sum_{i=1}^{n}(\xi_i + \xi_i')\right\}$$
$$\left\{\begin{array}{c} \langle \mathbf{w}, \psi(\mathbf{x}_i)\rangle + b - y_i \geq \varepsilon + \xi_i \\ y_i - (\langle \mathbf{w}, \psi(\mathbf{x}_i)\rangle + b) \geq \varepsilon + \xi_i' \\ \xi_i, \xi_i' \geq 0 \end{array}\right| \quad i = 1, \ldots, n \qquad (2)$$

where ξ_i, ξ_i', are slack variables that ensure that the solution does not contain, within the band of radius ε, all the points $(\mathbf{x}_i, y_i)$ of the sample (thus avoiding possible outliers and overfitting), where the parameter C expresses the importance of the slack variables in each point, and where $\psi : \mathcal{X} \rightarrow \mathcal{Z}$ is a transformation of the input space into a new space $\mathcal{Z}$ usually of larger dimension, where we define an inner product by means of a positive definite function k (kernel)

$$\langle \psi(\mathbf{x}), \psi(\mathbf{x}')\rangle = \sum_i \psi_i(\mathbf{x})\,\psi_i(\mathbf{x}') = k(\mathbf{x}, \mathbf{x}'). \qquad (3)$$

The kernel function can be linear, polynomial, radial basis, or sigmoidal. The linear and the polynomial kernel functions are used in problems without high nonlinearity; however, the sigmoid and the radial basis kernel functions are indicated for problems with high nonlinearity, as is the case of this research. Therefore, radial basis kernel function has been selected due to its better performance against the sigmoid kernel function.

The solution, which can be obtained from the dual problem, is a linear combination of a subset of sample points denominated

support vectors (s.v.) and it can be written as follows:

$$\mathbf{w} = \sum_{\text{s.v.}} \beta_i \psi(\mathbf{x_i}) \Rightarrow$$

$$f_{\mathbf{w},b}(\mathbf{x}) = \sum_{\text{s.v.}} \beta_i \langle \psi(\mathbf{x_i}), \psi(\mathbf{x}) \rangle + b = \sum_{\text{s.v.}} \beta_i k(\mathbf{x}_i, \mathbf{x}) + b. \quad (4)$$

It is possible to introduce a parameter in the SVM regression model (Nu-SVR) in order to control the number of support vectors determined [29].

A tenfold cross validation has been implemented in order to determine the optimal SVM parameters according to the best-fit criterion.

C. Linear Regression

The linear regression model can be formulated as follows:

$$\mathbf{Y} = a + \mathbf{bX} + \epsilon \quad (5)$$

where ϵ is the error to explain the variable $\mathbf{Y}$ by the hyperplane $a + \mathbf{bX}$. a, $\mathbf{b}$ are the constants of the regression model estimated from the sample data. In order to prove the nonlinearity of the problem, the results have been fitted by a linear regression. In addition, regression models were implemented between the explanatory variable and each predictor variables in order to establish the order of importance of each variable of the problem by analyzing the coefficient of determination

$$R^2 = 1 - \frac{\frac{1}{n}\sum_{i=1}^{n}(y_i - \widehat{y_i})^2}{S_Y^2} \quad (6)$$

where y_i, $\widehat{y_i}$ are the real and estimated values, respectively, and S_Y^2 is the variance of Y. The coefficient R^2 can assume values between 0 and 1 and it measures how good the estimated regression is.

IV. Results

A normalized variation of each parameter has been defined for all of the techniques. This parameter ν is obtained as $\nu = \frac{a - a_0}{a_1 - a_0}$, where the variable "$a$" represents each of the four parameters (lipid core length ν_l, lumen radius ν_r, fibrous cap thickness ν_{fc}, and lipid core width ν_w) in whatever position, and a_0 and a_1 are the lowest and highest values, respectively, of each parameter.

In order to predict the accuracy of the technique, the absolute of relative error (ER) and the correlation coefficient (RSQ) have been used

$$\text{ER} = \text{abs}\left(\frac{\widehat{\theta} - \theta}{\theta}\right) \quad (7)$$

$$\text{RSQ} = \frac{\sigma_{xy}}{\sigma_x \sigma_y} \quad (8)$$

where $\widehat{\theta}$ is the predicted MPS, θ is the real MPS, σ_{xy} is the covariance, and σ_x and σ_y are the standard deviations.

In the following, the results obtained by the different methods used in this study (linear regression, MLP, and SVM) are presented. Regarding simple regression, Table II shows the results of the coefficient R^2 for each simple regression model implemented between the explanatory variable and each predictor variable. Taking this data into account, we can conclude that the variable v_{fc} is the most influential of the explanatory variables since its coefficient is clearly the closest to 1.

TABLE II
Coefficients R^2 for the Different Predictor Variables

Variable	R^2
v_l	0.01506
v_r	0.01533
v_{fc}	0.7181
v_w	0.04774

TABLE III
ER and RSQ for the Linear Regression Model

		Test size 5	Test size 10
Test	RSQ	0.4792	0.4585
	ER	0.5458	0.5580

Henceforth, the results are calculated based on the test and train sets. The train set is used to generate the model; so, a high fit accurate (R^2 value closes to 1) in this set indicates that the model has been well trained, while the test set is used to validate it; therefore, a high fit accurate between the estimated and the actual values indicate that the model is appropriate to simulate the problem.

In order to strengthen the use of ANN and SVM techniques, the classical linear regression model has been included, and the results obtained are shown in Table III. Two test set sizes of 5 and 10 observations were used to contrast the different presented models, with the aim of deciding if the test size has influence in the error for each technique. The low value of RSQ and the high relative error of this model indicate the high nonlinearity of the problem and justify the use of these techniques.

In order to play up the importance of computational efficiency, the computational costs of the different methods studied can be compared. For the ANN and SVM, the computation train time is 7 ± 3 and 5 ± 2 min, respectively (once the optimal parameters have been chosen by tenfold cross validation and depending on the stopping criterion used), and the validation process time is negligible due to ANN and SVM techniques, which only evaluate a function, provided an immediate estimated response. However, once the FEM model has been constructed, the computational cost of each structural analysis is 10 ± 3 h.

The absolute of relative errors and the correlation coefficients for MLP and SVM techniques are shown in Tables IV and V, respectively. For the MLP technique, the optimum number of neurons in the hidden layer has been chosen by trial and error approach so that the error in prediction is minimized. In that case, the most accurate prediction has been for 100 neurons in the hidden layer neuron (test ER = 6.76% and RSQ = 0.9953). Increasing the number of neurons in the hidden layer increases the computation time, but the ER remains constant. However, decreasing the number of neurons in the hidden layer increases the ER. Conversely, for the SVM method, the Gaussian distribution with Nu-regression is the best combination (test ER = 4.14% and RSQ = 0.9997). In addition, SVM has greater updating capacity than the MLP, because once the model is generated and presented a new observation to itself, if the model is unable to estimate correctly the value, it simply adds this

TABLE IV
ER AND RSQ FOR THE MPL TECHNIQUE

		Test size 5				Test size 10	
	Neurons	50	75	100	150	100	150
Train	RSQ	0.965	0.978	0.9996	0.9995	0.9997	1
	ER	0.053	0.047	0.0013	0.0125	0.0112	0.0013
Test	RSQ	0.92	0.924	0.9953	0.9952	0.9513	0.9465
	ER	0.125	0.101	0.0676	0.0692	0.1097	0.1153

TABLE V
ER AND RSQ FOR THE SVM TECHNIQUE

		With Nu regression		Without Nu regression	
		Gaussian	*Normal*	*Gaussian*	*Normal*
Train	RSQ	1	1	1	1
	ER	5.13E-06	5.13E-06	0.000281	0.000281
Test	RSQ	0.9997	0.9997	0.9995	0.9995
	ER	0.041442	0.041442	0.073469	0.073469

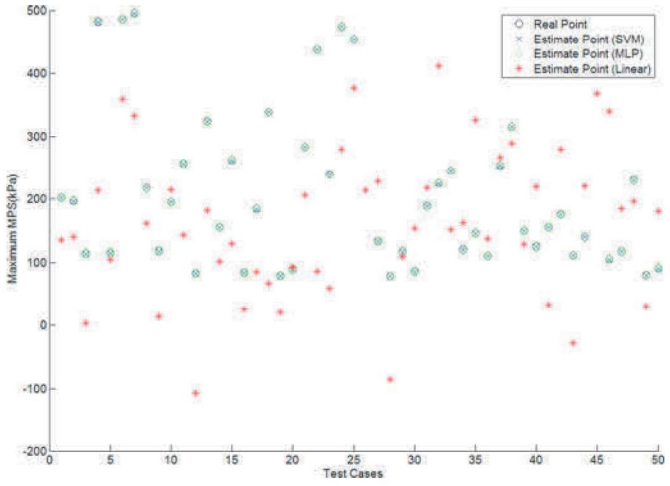

Fig. 4. Comparison of real points (o) and estimated points by linear regression (*), SVM (x) and MLP (◇) models in a set of 50 observations.

observation to the support vectors set without the need of a new training loop. However, MLP would need a new training to build a new model which includes information on the new observation presented.

In order to compare the results obtained by the three prediction methods, Fig. 4 shows the comparison of real points and estimated points by using linear regression, SVM, and MLP methods in a set of 50 observations. The SVM and MLP models present very accurate fits between the real and the estimated points with a high correlation between them. The results obtained by SVM are in fact even better than the MLP ones. However, the linear regression model provides a very poor fit between the real and estimated points.

V. DISCUSSION

Quantifying the mechanical stress in the wall of an atherosclerotic vessel and, more specifically, in the fibrous cap is a vital step in predicting the risk of plaque rupture based on biomechanical features. FEM is playing an increasing role in medical practice, being used in preoperatory surgical planning when clinical staff have enough time to perform the computational model and analyze the results. However, FEM presents the disadvantage of very high computational cost. From the results of this study, we can conclude that both ANN and SVM techniques represent a powerful tool to replace FEM simulations used in cardiovascular mechanics to quantify the vulnerable risk since they provide an immediate response and the relative errors obtained are less than 10% for both methods.

The presence of high nonlinearities in the problem, as reflected by the results of classical linear regression model, reinforces the use of such alternative techniques to solve the regression problem. It was demonstrated that the SVM technique used in this study has the capacity to produce higher overall prediction accuracy than a particular specific MLP architecture since the relative error obtained is 4.14% and 6.76% in the SVM and ANN techniques, respectively. Based on this observation, we could conclude that SVM represents a useful method for vulnerable atheroma plaque detection. On the contrary, linear regression is not an appropriate technique to solve this problem due to the extremely high relative error obtained (55%).

A particular advantage of SVM is that a SVM classifier depends only on the support vectors, and the classifier function is not influenced by the whole dataset, as it is the case for many neural network systems. Additionally, SVMs are faster in training, but requires an appropriate choice of kernel function and parameters.

Some limitations of this study should also be mentioned. First, an idealized straight geometry has been used to perform the parametric analysis; thus, the local curvature and other features such as the blood pressure have not been considered. Second, the material constitutive properties has not been considered. However, these assumptions have been widely accepted as allowable for the assessment of the biomechanical properties of atherosclerotic lesions [22]. Third, global RS has been considered since there is any technique to measure the RS pointwise. Fourth, a huge set of real clinical data should be used in conjunction with the data obtained from the idealized geometry to train the ANN or SVM in order to quantitatively validate the results.

Despite these limitations, and according to the results obtained, we come to the following conclusion; the ANN and SVM techniques are able to replace FEM simulations to predict the maximum MPS on an idealized coronary model with a good error tolerance and avoiding the time-consuming 3-D FE analysis. However, the use of both techniques, FEM and MLT, in clinical practice remains unclear because it is necessary to clarify the real role of stress in plaque vulnerability and to perform a quantitative validation with clinical data.

REFERENCES

[1] H. Hanke, C. Lenz, and G. Finking, "The discovery of the pathophysiological aspects of atherosclerosis—A review," *Acta Chirurgica Belgica*, vol. 101, pp. 162–169, 2001.

[2] J. G. Kips, P. Segers, and L. M. Van Bortel, "Identifying the vulnerable plaque: A review of invasive and non-invasive imaging modalities," *Artery Res.*, vol. 2, pp. 21–34, 2008.

[3] M. Naghavi and E. Falk, *From Vulnerable Plaque to Vulnerable Patient* (ser. Contemporary Cardiology), M. Naghavi, Ed. New York: Humana Press, 2010.

[4] A. Versluis, A. J. Bank, and W. H. Douglas, "Fatigue and plaque rupture in myocardial infarction," *J. Biomech.*, vol. 39, pp. 339–347, 2006.

[5] R. Virmani, F. D. Kolodgie, A. P. Burke, A. Farb, and S. M. Schwartz, "Lessons from sudden coronary death: A comprehensive morphological

classification scheme for atherosclerotic lesions," *Arterioscler., Thromb., Vascul. Biol.*, vol. 20, pp. 1262–1275, 2000.

[6] R. K. Kumar and K. R. Balakrishnan, "Influence of lumen shape and vessel geometry on plaque stresses: Possible role in the increased vulnerability of a remodelled vessel and the shoulder of a plaque," *Heart*, vol. 91, pp. 1459–1465, 2005.

[7] M. Cilla, E. Peña, and M. Martinez, "3D computational parametric analysis of eccentric atheroma plaque. Influence of axial residual stresses," *Biomech. Model. Mechanobiol.*, 2011. In Press, doi:10.1007/s10237-011-0369-0.

[8] V. Vapnik, *Estimation of Dependences Based on Empirical Data*. New York: Springer-Verlag, 1982.

[9] B. Scholkpof and A. Smola, *Learning With Kernels: Support Vector Machines, Regularization, Optimization, and Beyond*. Cambridge, MA: MIT Press, 2002.

[10] C. Bishop, *Neural Networks and Pattern Recognition*. Oxford, U.K.: Oxford Univ. Press, 1995.

[11] J. Taboada, J. Matias, C. Ordoñez, and P. Garcia, "Creating a quality map of a slate deposit using support vector machines," *J. Comput. Appl. Math.*, vol. 204, pp. 84–94, 2007.

[12] M. Lopez, J. Martinez, J. Matías, J. Taboada, and J. Vilan, "Shape functional optimization with restrictions boosted with machine learning techniques," *J. Comput. Appl. Math.*, vol. 234, pp. 2609–2615, 2010.

[13] M. Lopez, J. Martinez, J. Matias, J. Taboada, and J. Vilan, "Functional classification of ornamental stone using machine learning techniques," *J. Comput. Appl. Math.*, vol. 234, pp. 1338–1345, 2010.

[14] M. J. Davies, "Stability and instability: Two faces of coronary atherosclerosis: The Paul Dudley White lecture 1995," *Circulation*, vol. 94, pp. 2013–2020, 1996.

[15] J. Ohayon, P. Teppaz, G. Finet, and G. Rioufol, "In-vivo prediction of human coronary plaque rupture location using intravascular and finite element method," *Coronary Artery Disease*, vol. 12, pp. 655–663, 2001.

[16] G. Finet, J. Ohayon, and G. Rioufol, "Biomechanical interaction between cap thickness, lipid core composition and blood pressure in vulnerable coronary plaque: Impact on stability or instability," *Coronary Artery Disease*, vol. 15, pp. 13–20, 2004.

[17] D. Bluestein, Y. Alemu, I. Avrahami, M. Gharib, K. Dumont, J. J. Ricotta, and S. Einav, "Influence of microcalcifications on vulnerable plaque mechanics using FSI modelling," *J. Biomech.*, vol. 41, pp. 1111–1118, 2008.

[18] G. A. Holzapfel, C. T. Gasser, G. Sommer, and P. Regitnig, "Determination of the layer-specific mechanical properties of human coronary arteries with non-atherosclerotic intimal thickening, and related constitutive modelling," *Amer. J. Physiol. Heart Circ. Physiol.*, vol. 289, pp. H2048–H2058, 2005.

[19] T. C. Gasser, R. W. Ogden, and G. A. Holzapfel, "Hyperelastic modelling of arterial layers with distributed collagen fibre orientations," *J. Roy. Soc. Interface*, vol. 3, pp. 15–35, 2006.

[20] D. W. Marquardt, "An algorithm for least-squares estimation of nonlinear parameters," *SIAM J. Appl. Math.*, vol. 11, pp. 431–441, 1963.

[21] J. Ohayon, G. Finet, A. M. Gharib, D. A. Herzka, P. Tracqui, J. Heroux, G. Rioufol, M. S. Kotys, A. Elagha, and R. I. Pettigrew, "Necrotic core thickness and positive arterial remodeling index: Emergent biomechanical factors for evaluating the risk of plaque rupture," *Amer. J. Physiol. Heart Circ. Physiol.*, vol. 295, pp. H717–H727, 2008.

[22] G. Cheng, H. Loree, R. Kamm, M. Fishbein, and R. Lee, "Distribution of circumferential stress in ruptured and stable atherosclerotic lesions. A structural analysis with histopathological correlation," *Circulation*, vol. 87, pp. 1179–1187, 1993.

[23] S. D. Williamson, Y. Lam, H. F. Younis, H. Huang, S. Patel, M. R. Kaazempur-Mofrad, and R. D. Kamm, "On the sensitivity of wall stresses in diseased arteries to variable material properties," *ASME J. Biomech. Eng.*, vol. 125, pp. 147–155, 2003.

[24] K. Fujii, S. G. Carlier, G. S. Mintz, W. Wijns, A. Colombo, D. Böse, R. Erbel, J. de Ribamar Costa, Jr., M. Kimura, K. Sano, R. A. Costa, J. Lui, G. W. Stone, J. W. Moses, and M. B. Leon, "Association of plaque characterization by intravascular ultrasound virtual histology and arterial remodeling," *Amer. J. Cardiol.*, vol. 96, pp. 1476–1483, 2005.

[25] H. M. Loree, A. J. Grodzinsky, S. Y. Park, L. J. Gibson, and R. T. Lee, "Static circumferential tangential modulus of human atherosclerotic tissue," *J. Biomech.*, vol. 27, pp. 195–204, 1994.

[26] W. MacCulloch and W. Pitts, "A logical calculus of the ideas inmanent in nervous activity," *Bull. Math. Biophys.*, vol. 5, pp. 115–133, 1943.

[27] M. Stone, "Cross-validatory choice and assessment of statistical predictions," *J. Roy. Statist. Soc. Series B*, vol. 36, pp. 111–147, 1974.

[28] H. Drucker, C. Burges, L. Kaufman, A. Smola, and V. Vapnik, *Support Vector Regression Machines*. Cambridge, MA: MIT Press, 1997.

[29] B. Scholkopf, A. J. Smola, R. C. Williamson, and P. L. Bartlett, "New support vector algorithms," *Neural Comput.*, vol. 12, pp. 1207–1245, 2000.